

Dalton Transaction - Full Article

Bis(6-diphenylphosphinoacenaphth-5-yl)telluride as Ligand

Towards Coinage Metal Chlorids

Truong Giang Do,^a Emanuel Hupf,^{a,b} Enno Lork,^a Stefan Mebs,^c* Jens Beckmann^a*

^a *Institut für Anorganische Chemie, Universität Bremen, Leobener Straße, 28359 Bremen, Germany*

^b *Department of Chemistry, University of Alberta, 11227 Saskatchewan Dr., Edmonton, Alberta,
T6G 2G2, Canada*

^c *Institut für Experimentalphysik, Freie Universität Berlin, Arnimallee 14, 14195 Berlin, Germany*

Supporting Information

Contents

Experimental Section

Figure S1a ¹H-NMR spectrum of **7** (CD₂Cl₂).

Figure S1b ¹³C {¹H}-NMR spectrum of **7** (CD₂Cl₂).

Figure S1c ³¹P {¹H}-NMR spectrum of **7** (CD₂Cl₂).

Figure S1d ¹²⁵Te {¹H}-NMR spectrum of **7** (CD₂Cl₂).

Figure S2a ¹H-NMR spectrum of **8** (CD₂Cl₂).

Figure S2b ¹³C {¹H}-NMR spectrum of **8** (CD₂Cl₂).

Figure S2c ³¹P {¹H}-NMR spectrum of **8** (CD₂Cl₂).

Figure S2d ¹²⁵Te {¹H}-NMR spectrum of **8** (CD₂Cl₂).

* Correspondence to Jens Beckmann (E-mail: j.beckmann@uni-bremen.de) and Stefan Mebs (E-mail: steb@chemie.fu-berlin.de)

- Figure S3a** ^1H -NMR spectrum of **12** (CD_2Cl_2).
- Figure S3b** $^{13}\text{C}\{^1\text{H}\}$ -NMR spectrum of **12** (CD_2Cl_2).
- Figure S3c** $^{31}\text{P}\{^1\text{H}\}$ -NMR spectrum of **12** (CD_2Cl_2).
- Figure S3d** $^{125}\text{Te}\{^1\text{H}\}$ -NMR spectrum of **12** (CD_2Cl_2).
- Figure S4** The molar conductivity of **12** in CH_2Cl_2 .

DFT calculations

- Table S1** Topological and integrated bond descriptors of relevant bonds.
- Figure S5** Labelling scheme for (a) **6**, (b) **7**, (c) **8**.
- Figure S6** Labelling scheme for (a) **12**, (b) **13**.

Experimental Section

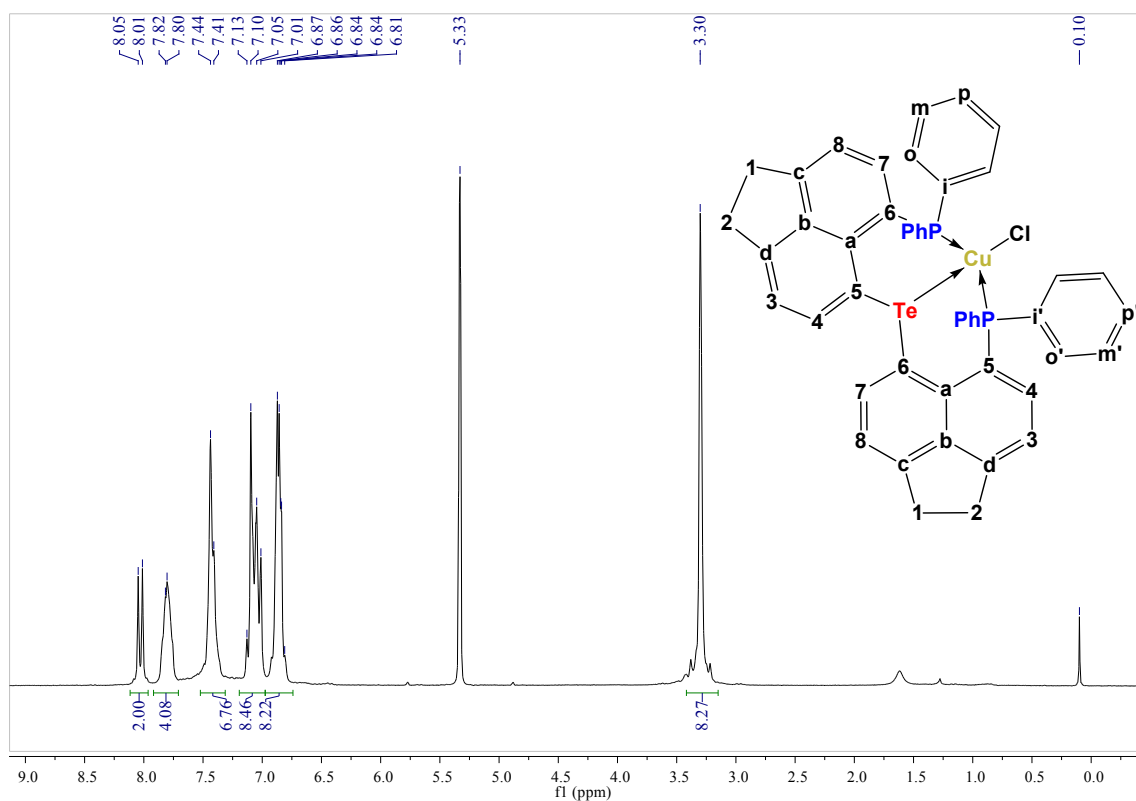


Figure S1a: $^1\text{H-NMR}$ spectrum (CD_2Cl_2) of **7**.

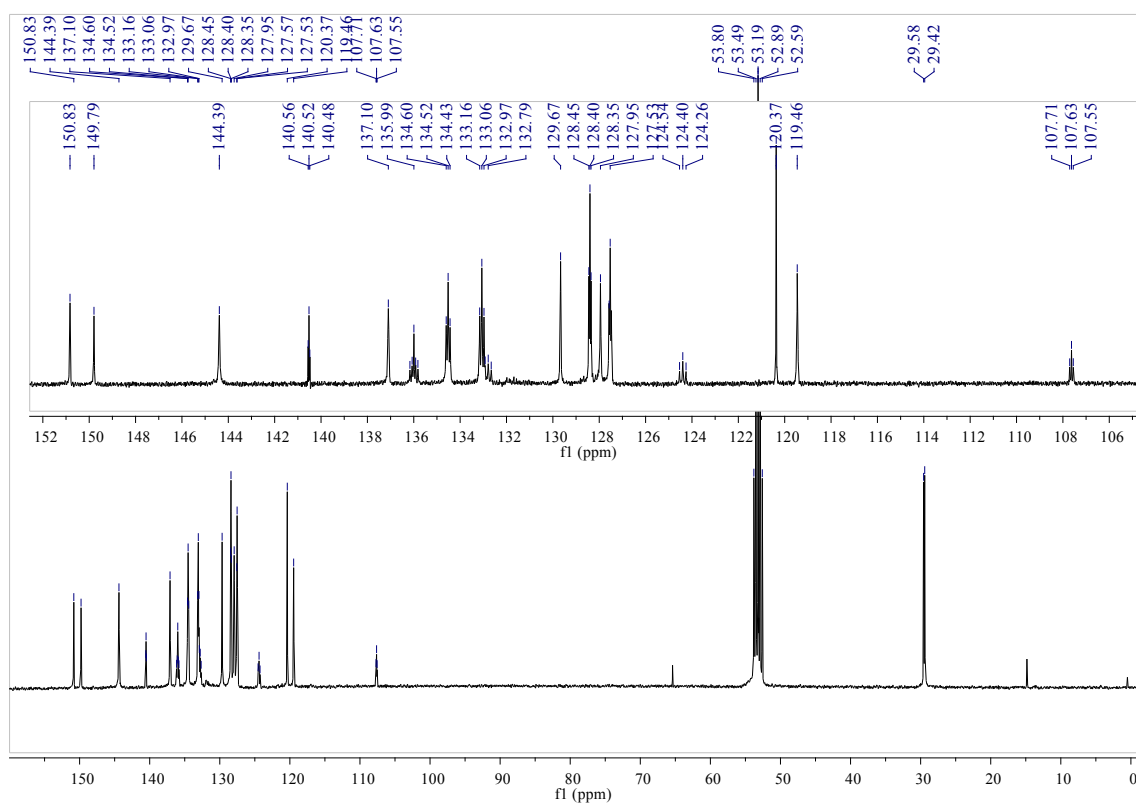


Figure S1b: $^{13}\text{C}\{^1\text{H}\}$ -NMR spectrum (CD_2Cl_2) of **7**.

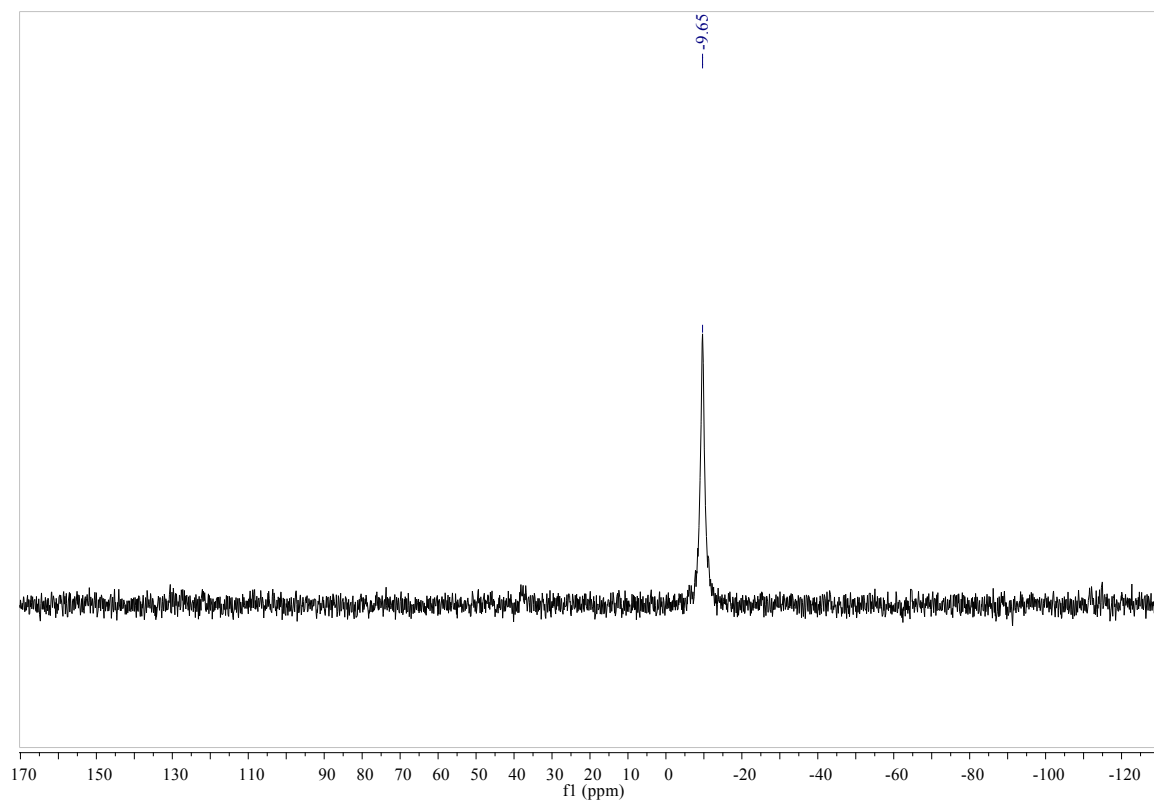


Figure S1c: $^{31}\text{P}\{^1\text{H}\}$ -NMR spectrum (CD_2Cl_2) of **7**.

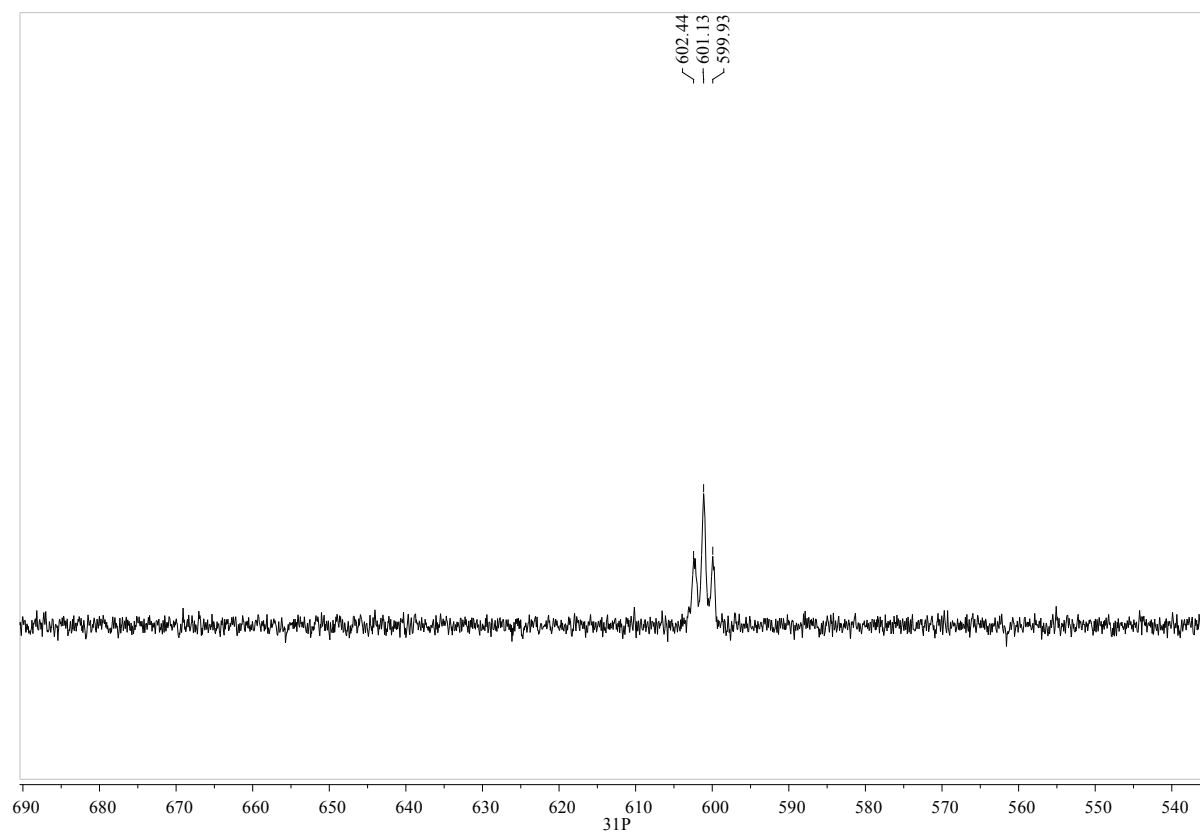


Figure S1d: $^{125}\text{Te}\{^1\text{H}\}$ -NMR spectrum (CD_2Cl_2) of **7**.

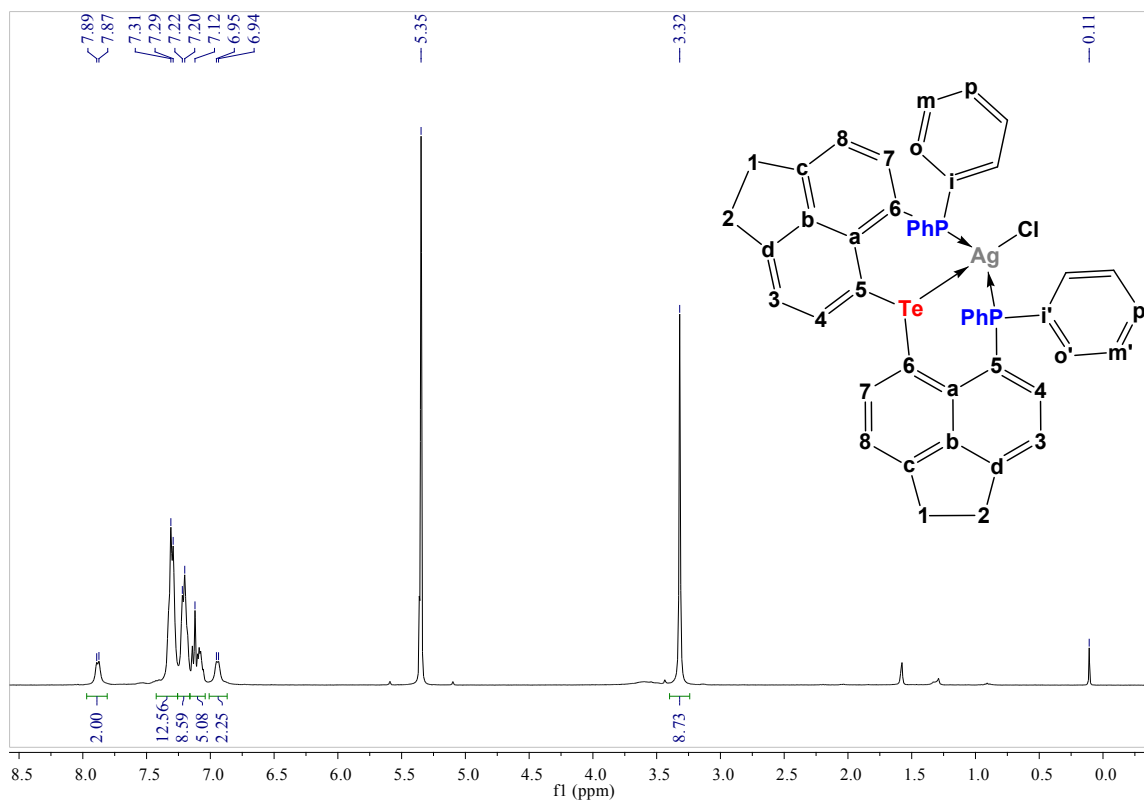


Figure S2a. ¹H-NMR spectrum (CD₂Cl₂) of **8**.

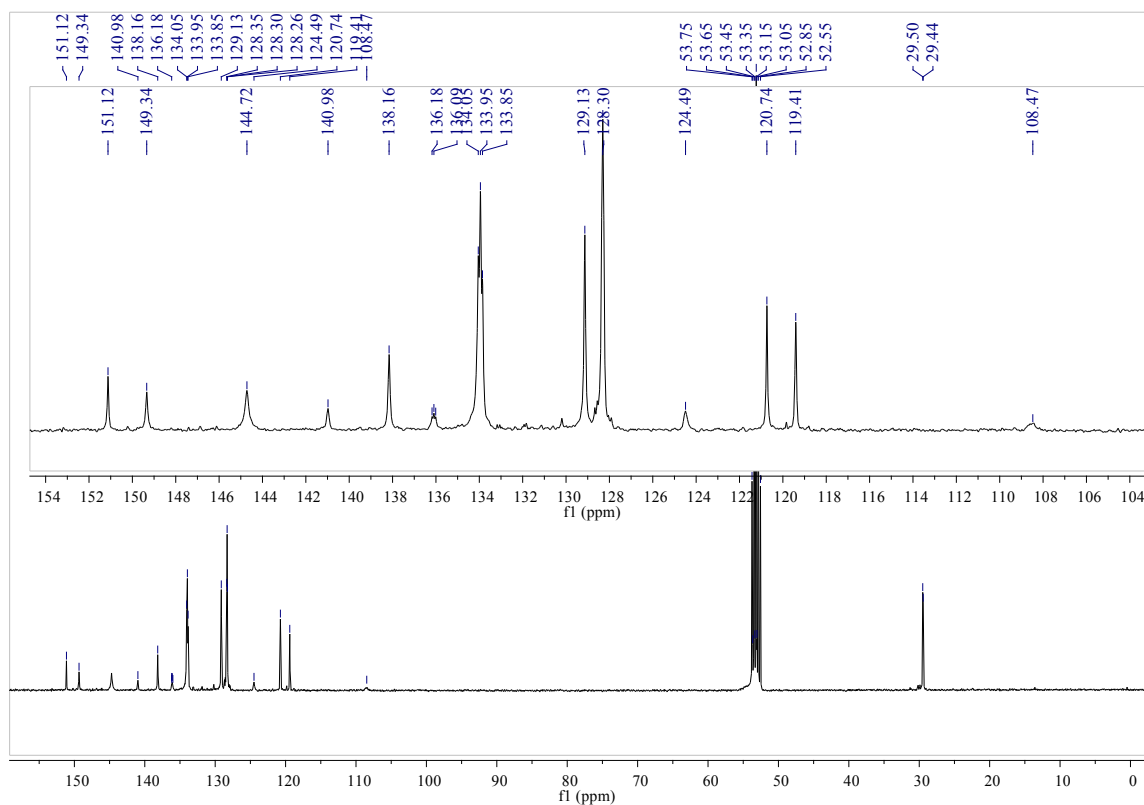


Figure S2b. ¹³C{¹H}-NMR spectrum (CD₂Cl₂) of **8**.

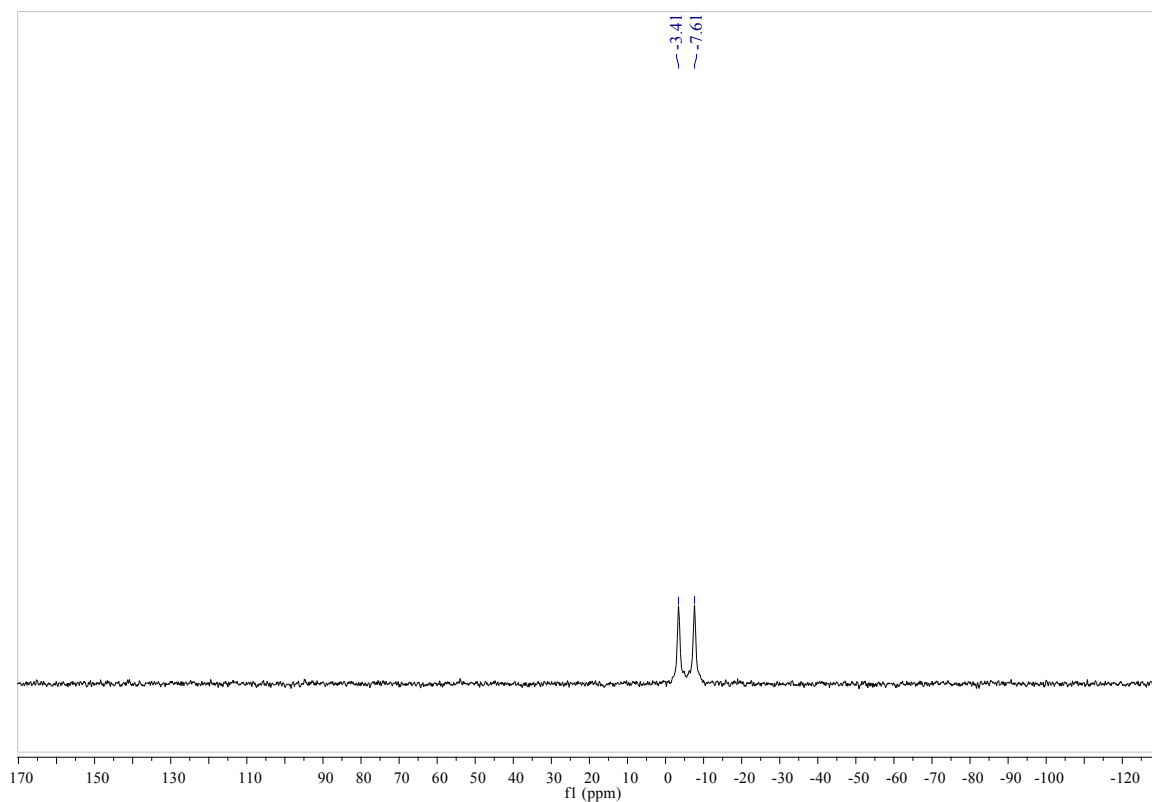


Figure S2c: $^{31}\text{P}\{^1\text{H}\}$ -NMR spectrum (CD_2Cl_2) of **8**.

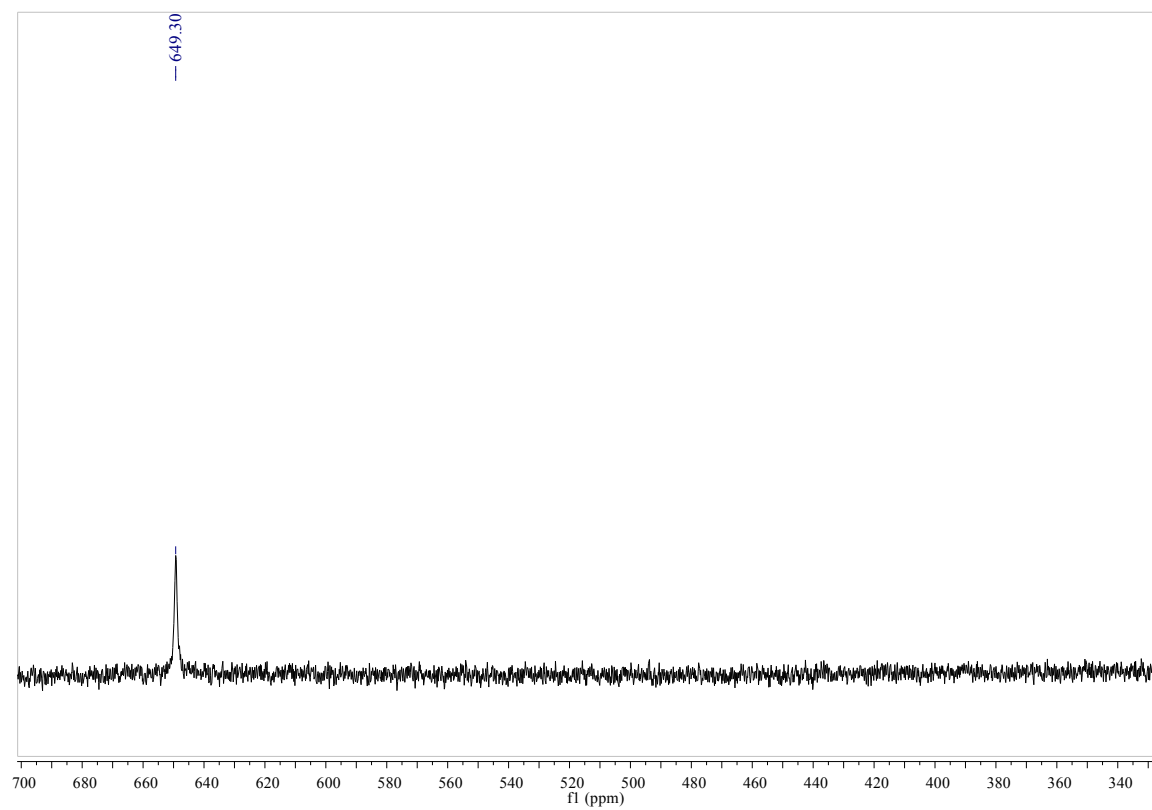


Figure S2d: $^{125}\text{Te}\{^1\text{H}\}$ -NMR spectrum (CD_2Cl_2) of **8**.

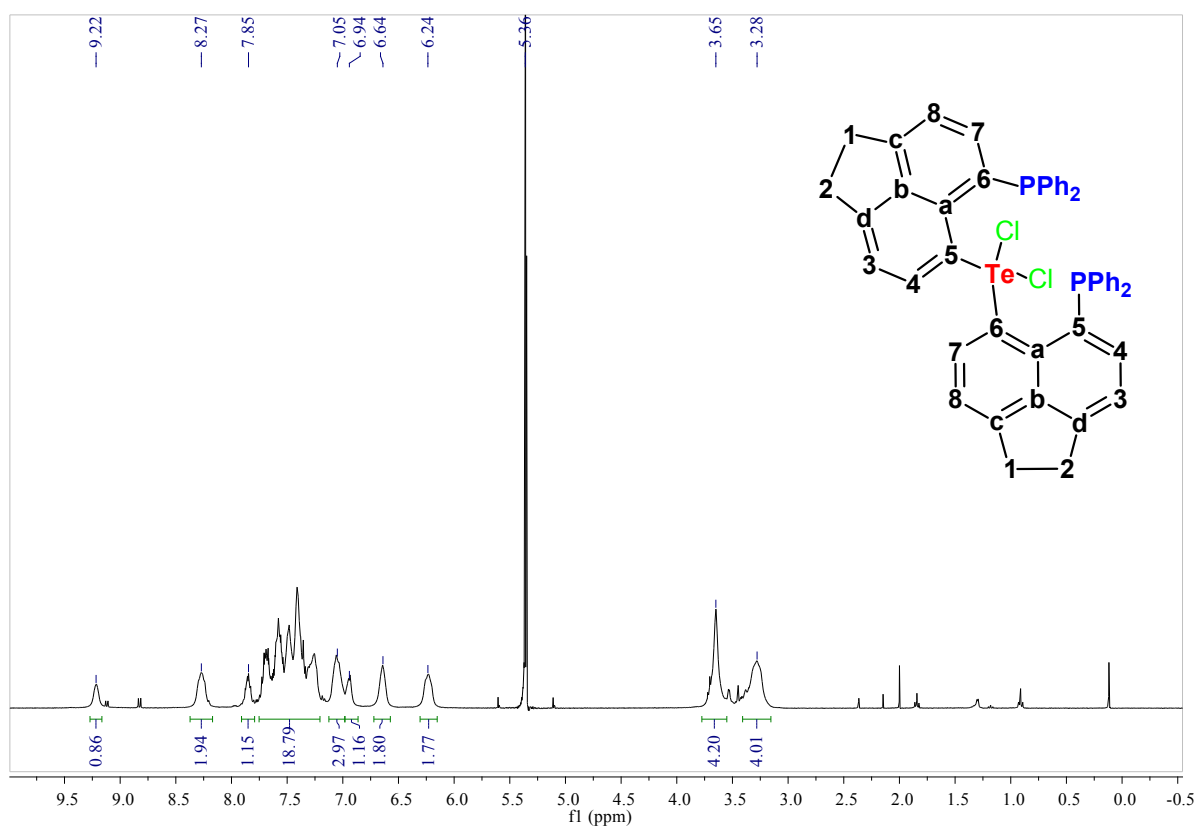


Figure S3a. ¹H-NMR spectrum (CD₂Cl₂) of 12.

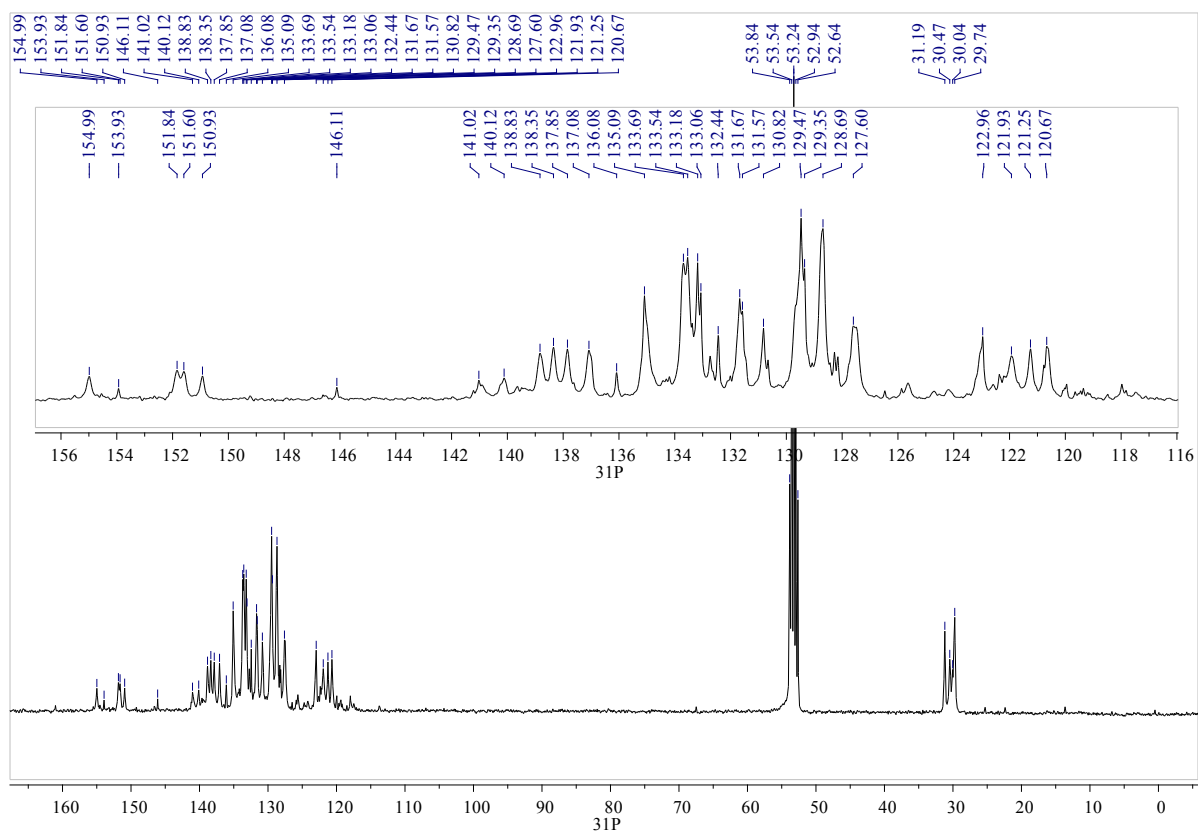


Figure S3b. ¹³C{¹H}-NMR spectrum (CD₂Cl₂) of 12.

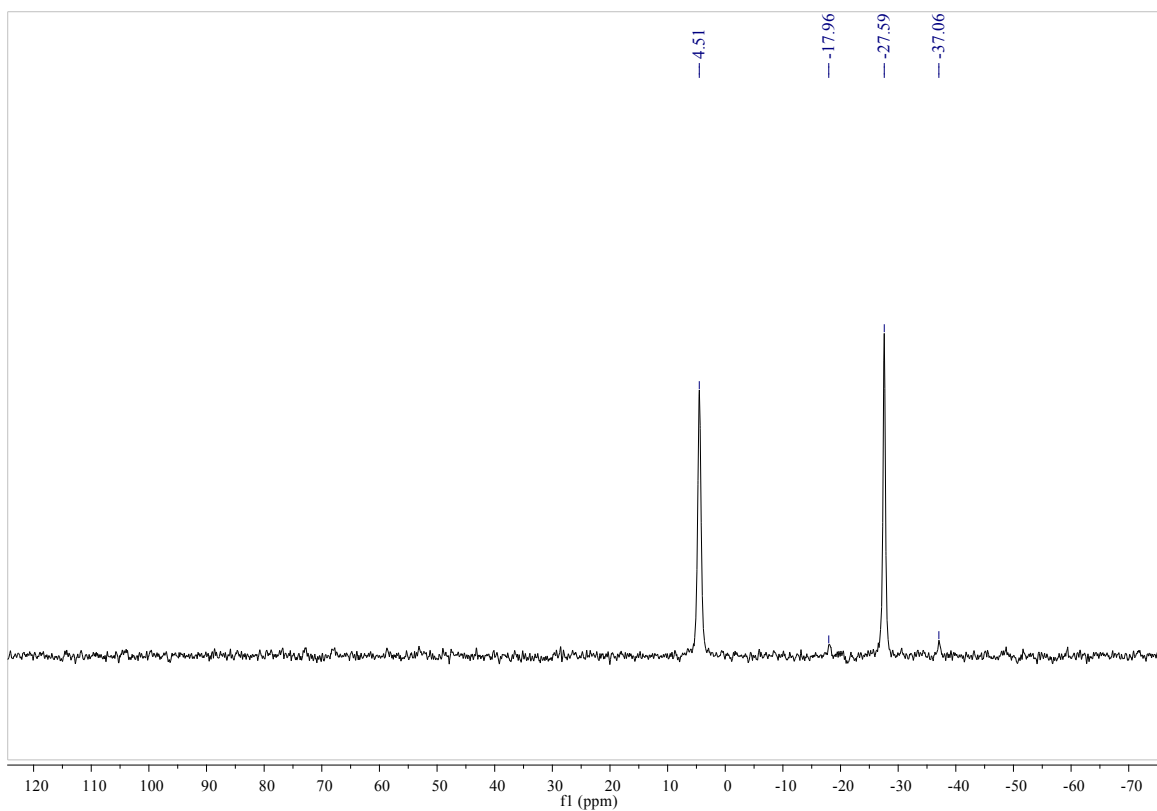


Figure S3c. $^{31}\text{P}\{^1\text{H}\}$ -NMR spectrum (CD_2Cl_2) of **12**.

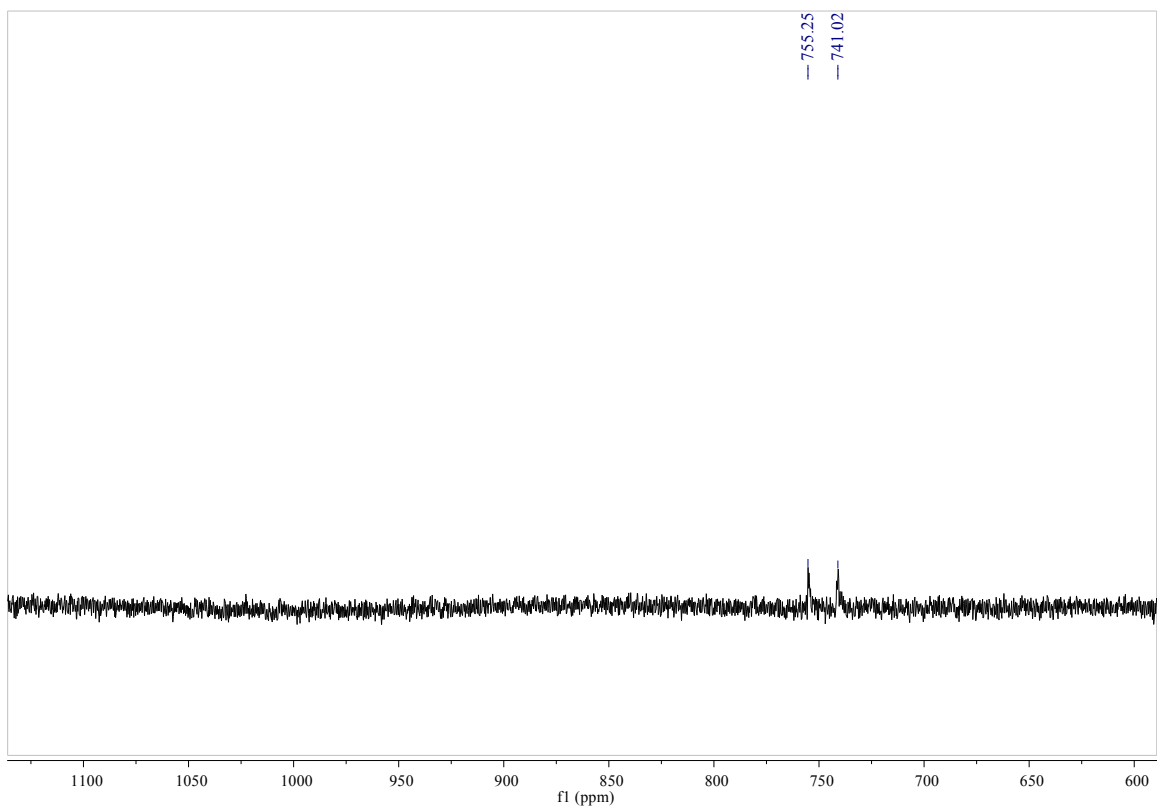


Figure S3d. $^{125}\text{Te}\{^1\text{H}\}$ -NMR spectrum (CD_2Cl_2) of **12**.

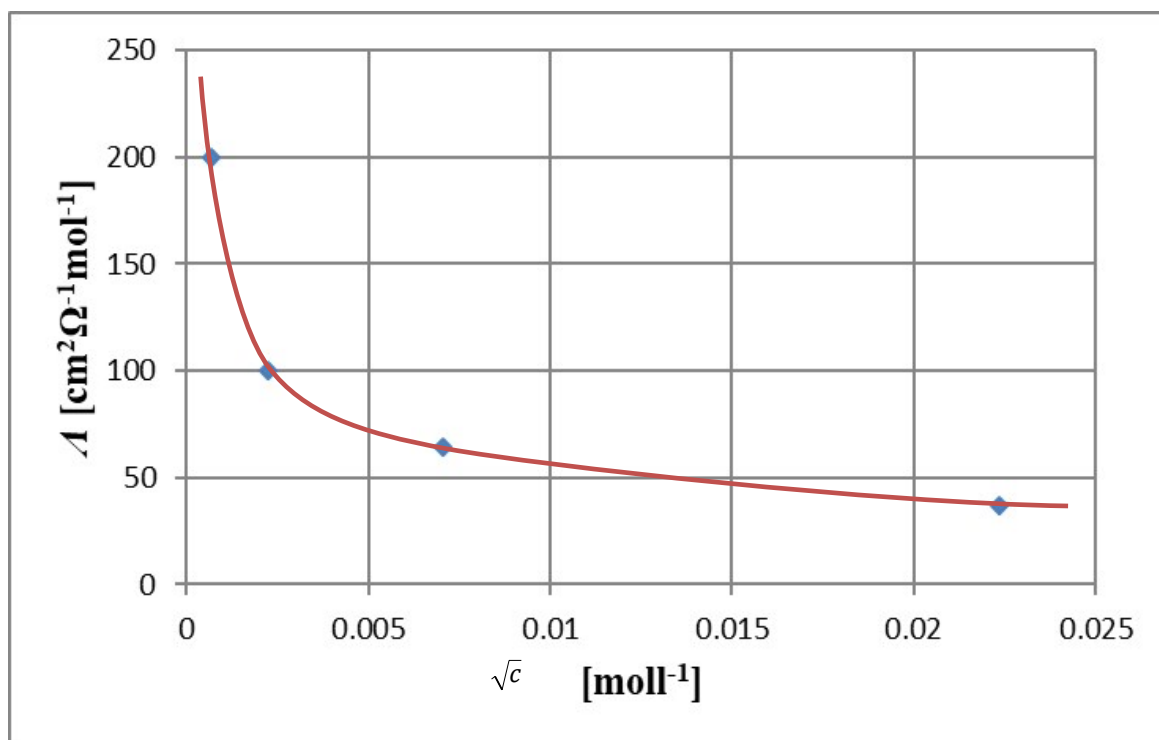
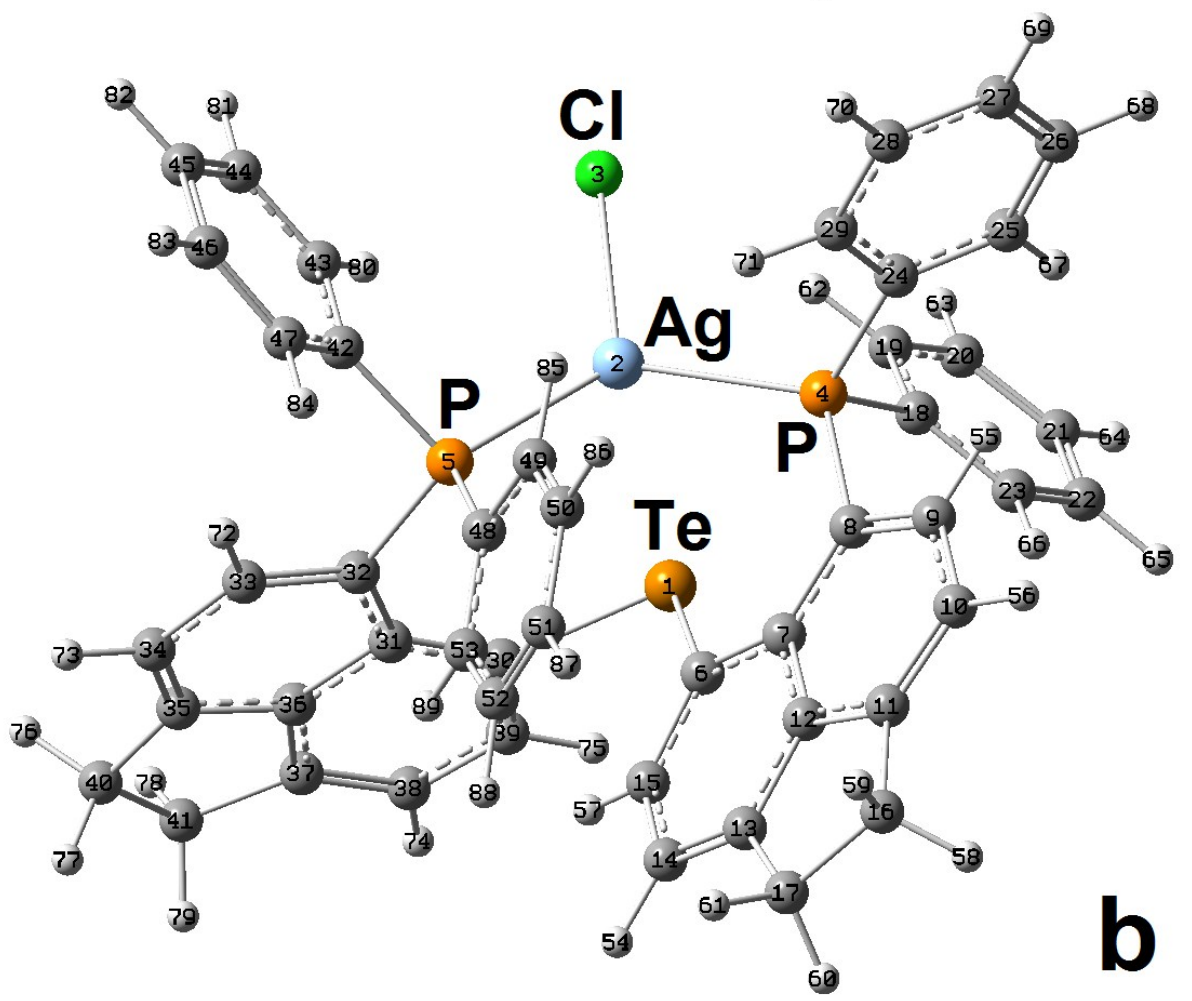
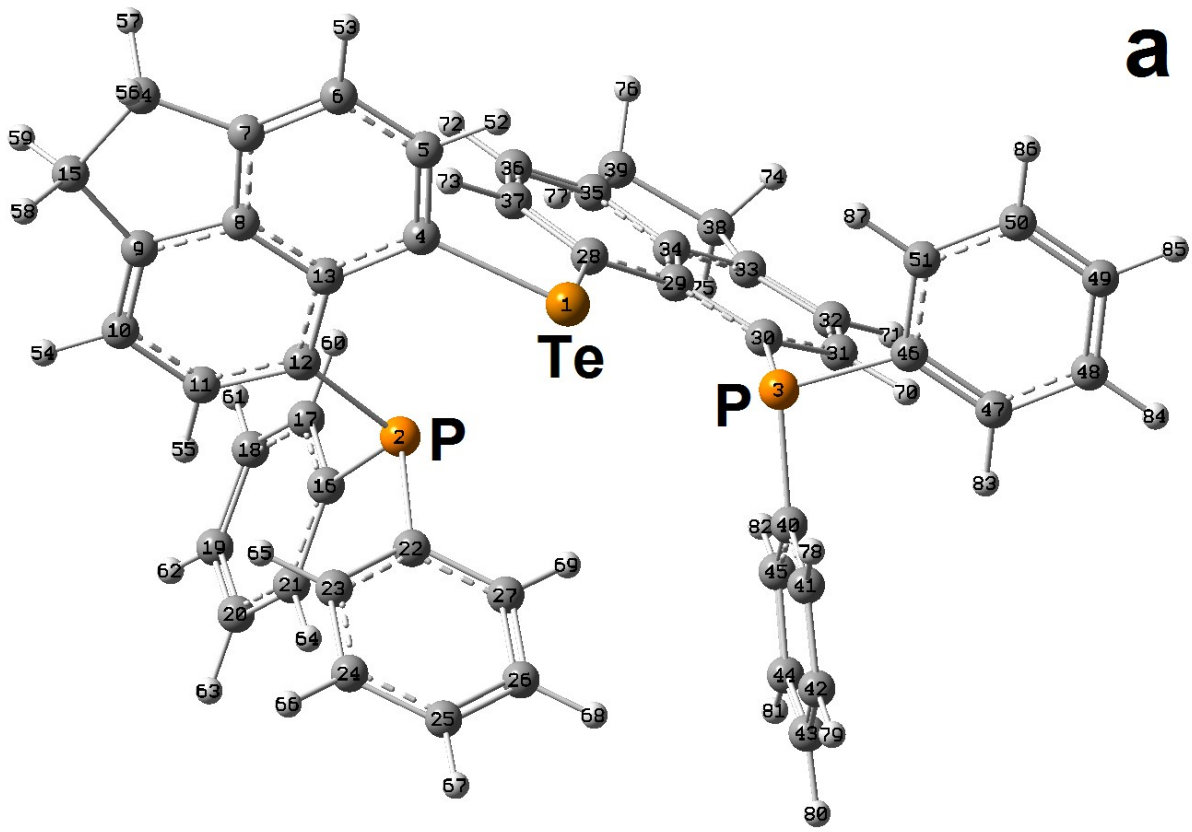


Figure S4. The molar conductivity of **12** in CH_2Cl_2

Table S1. Topological and integrated bond descriptors of relevant bonds of **6**, **7**, **8**, **12'** and **13'**

	bond	d_1+d_2 [Å]	$\rho(\mathbf{r})_{\text{bcp}}$ [eÅ ⁻³]	$\nabla^2\rho(\mathbf{r})_{\text{bcp}}$ [eÅ ⁻⁵]	$G/\rho(\mathbf{r})_{\text{bcp}}$ [a.u.]	$H/\rho(\mathbf{r})_{\text{bcp}}$ [a.u.]	N_{ELI} [e]	V_{ELI} [Å ³]	Y_{max}	Δ_{ELI} [Å]	RJI [%]
6	Te-P2	3.369	0.13	0.7	0.42	-0.04	2.09	13.5	2.46	LP	98.3
	Te-P3	3.137	0.18	0.9	0.46	-0.09	2.04	13.1	2.31	LP	97.8
	Te-C4	2.158	0.77	0.1	0.52	-0.50	2.04	5.4	1.71	0.142	74.9
	Te-C28	2.143	0.79	-0.3	0.49	-0.51	1.94	5.0	1.68	0.031	71.8
7	Te-Cu	2.558	0.40	2.6	0.73	-0.27	2.18	10.4	1.33	0.804	79.3
	LP(Te)	-	-	-	-	-	2.49	19.5	1.88	LP	-
	Cu-Cl	2.256	0.50	5.4	1.03	-0.27	0.43	0.6	1.49	0.009	88.7
	Cu-P4	2.215	0.60	4.0	0.84	-0.37	2.52	13.3	1.69	0.288	73.1
	Cu-P5	2.234	0.58	3.9	0.84	-0.36	2.40	11.0	1.73	0.348	77.1
	Te-C6	2.124	0.82	-0.2	0.51	-0.53	2.03	5.6	1.69	0.138	71.8
	Te-C30	2.144	0.79	-0.3	0.49	-0.52	1.98	5.5	1.68	0.067	71.1
8	Te-Ag	2.877	0.29	2.0	0.66	-0.17	2.17	11.9	1.41	LP	93.9
	LP(Te)	-	-	-	-	-	2.36	18.5	1.88	LP	-
	Ag-Cl	2.463	0.43	4.4	0.93	-0.21				no ELI-D basin	
	Ag-P4	2.462	0.49	3.2	0.76	-0.29	2.12	10.6	1.78	0.356	85.6
	Ag-P5	2.429	0.51	3.5	0.78	-0.31	2.13	10.3	1.74	0.330	84.9
	Te-C6	2.146	0.79	-0.4	0.48	-0.51	1.97	5.3	1.68	0.087	70.8
	Te-C30	2.125	0.82	-0.2	0.51	-0.52	2.01	5.3	1.68	0.131	71.1
12'	Te-Cl	2.619	0.41	1.3	0.49	-0.27				no ELI-D basin	
	Te-P3	2.654	0.48	-0.2	0.32	-0.35	2.01	7.9	1.91	0.158	76.1
	Te-P4	3.186	0.17	0.8	0.40	-0.09	2.02	12.8	2.35	LP	97.6
	Te-C9	2.145	0.82	-1.0	0.44	-0.53	2.15	5.9	1.66	0.130	64.0
	Te-C31	2.157	0.80	-1.5	0.39	-0.52	2.09	5.7	1.65	0.053	57.7
13'	Te-Cl	2.443	0.56	1.3	0.55	-0.39				no ELI-D basin	
	Te-N3	2.442	0.41	1.9	0.56	-0.23	2.08	4.2	1.82	LP	95.1
	Te-N4	2.799	0.22	1.4	0.52	-0.07	2.12	4.9	1.91	LP	99.6
	Te-C9	2.141	0.83	-1.2	0.43	-0.54	2.16	5.9	1.67	0.057	63.1
	Te-C19	2.146	0.82	-1.6	0.40	-0.53	2.18	6.2	1.66	0.038	58.4

For all bonds, d_1 and d_2 are the distances of the atoms to the bcp, $\rho(\mathbf{r})_{\text{bcp}}$ is the electron density at the bond critical point, $\nabla^2\rho(\mathbf{r})_{\text{bcp}}$ is the corresponding Laplacian, $G/\rho(\mathbf{r})_{\text{bcp}}$ and $H/\rho(\mathbf{r})_{\text{bcp}}$ are the kinetic and total energy density over $\rho(\mathbf{r})_{\text{bcp}}$ ratios, N_{ELI} and V_{ELI} are the electron population and volume of the ELI-D basin, Y_{max} is the ELI-D value at the attractor position, Δ_{ELI} is the distance of the attractor position to the atom-atom axis, RJI is the Raub-Jansen Index. For labelling, see Figures S5 and S9.



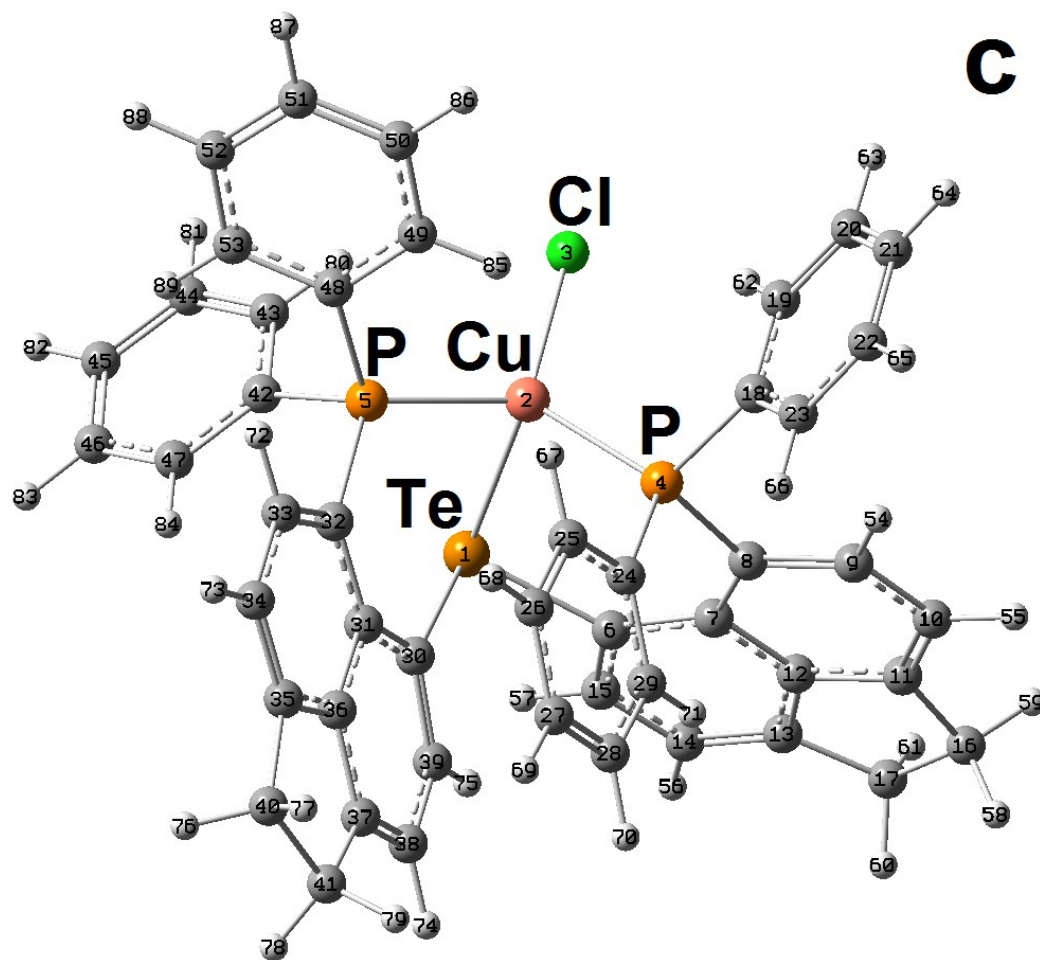


Figure S5. Labelling scheme for (a) 6, (b) 7, (c) 8.

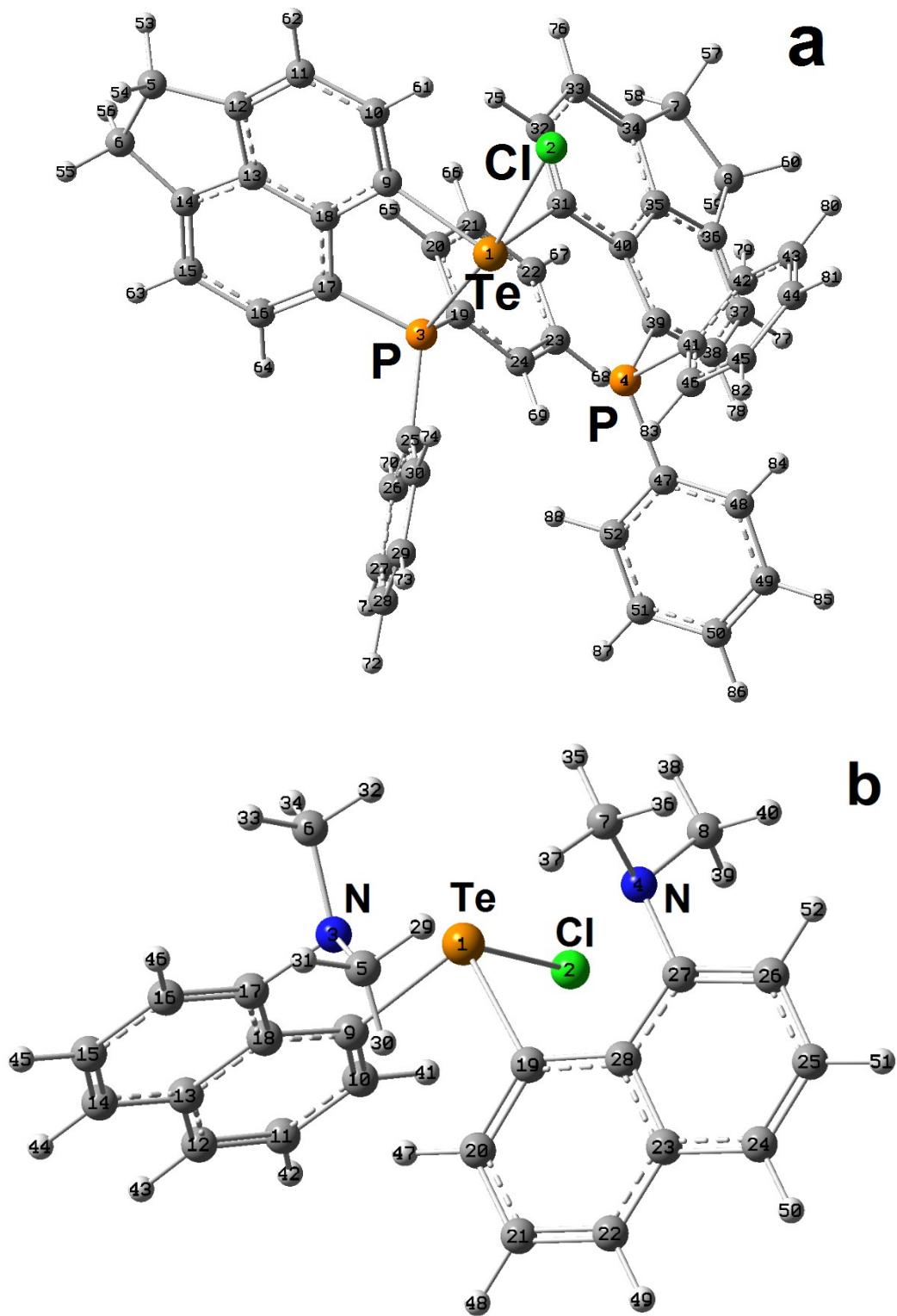


Figure S6. Labelling scheme for (a) 12', (b) 13'.